Received: 27 May 2019 | Revised: 10 May 2020 | Accepted: 14 May 2020

DOI: 10.1111/bph.15146

RESEARCH PAPER

Silencing of spontaneous activity at α4β1/3δ $GABA_A$ receptors in hippocampal granule cells reveals different ligand pharmacology

Nils Ole Dalby[1] | Christina Birkedahl Falk-Petersen[1] | Ulrike Leurs[1] | Petra Scholze[2] | Jacob Krall[1] | Bente Frølund[1] | Petrine Wellendorph[1]

[1]Department of Drug Design and Pharmacology, Faculty of Health and Medical Sciences, University of Copenhagen, Copenhagen, Denmark

[2]Department of Pathobiology of the Nervous System, Center for Brain Research, Medical University of Vienna, Vienna, Austria

Correspondence
Nils Ole Dalby and Petrine Wellendorph, Department of Drug Design and Pharmacology, Faculty of Health and Medical Sciences, University of Copenhagen, Universitetsparken 2, DK-2100 Copenhagen, Denmark.
Email: nilbys@gmail.com; pw@sund.ku.dk

Funding information
Lundbeck Foundation, Grant/Award Numbers: R133-A12270, R192-2015-666, R230-2016-2562

Background and Purpose: The δ-subunit-containing $GABA_A$ receptors, $\alpha_4\beta_1\delta$ and $\alpha_4\beta_3\delta$, in dentate gyrus granule cells (DGGCs) are known to exhibit both spontaneous channel openings (i.e. constitutive activity) and agonist-induced current. The functional implications of spontaneous gating are unclear. In this study, we tested the hypothesis that constitutively active $\alpha_4\beta_{1/3}\delta$ receptors limit agonist efficacy.

Experimental Approach: Whole-cell electrophysiological recordings of adult male rat and mouse hippocampal DGGCs were used to characterize known agonists and antagonists at δ-subunit-containing $GABA_A$ receptors. To separate constitutive and agonist-induced currents, different recording conditions were employed.

Key Results: Recordings at either 24°C or 34°C, including the PKC autoinhibitory peptide (19–36) intracellularly, removed spontaneous gating by $GABA_A$ receptors. In the absence of spontaneous gating, DGGCs responded to the $\alpha_4\beta_{1/3}\delta$ orthosteric agonist Thio-THIP with a four-fold increased efficacy relative to recording conditions favouring constitutive activity. Surprisingly, the neutral antagonist gabazine was unable to antagonize the current by Thio-THIP. Furthermore, a current was elicited by gabazine alone only when the constitutive current was silenced (EC_{50} 2.1 μM). The gabazine-induced current was inhibited by picrotoxin, potentiated by DS2, completely absent in $\delta^{-/-}$ mice and reduced in $\beta_1{}^{-/-}$ mice, but could not be replicated in human $\alpha_4\beta_{1/3}\delta$ receptors expressed heterologously in HEK cells.

Conclusion and Implications: Kinase activity infers spontaneous gating in $\alpha_4\beta_{1/3}\delta$ receptors in DGGCs. This significantly limits the efficacy of $GABA_A$ agonists and has implications in pathologies involving aberrant excitability caused by phosphorylation (e.g. addiction and epilepsy). In such cases, the efficacy of δ-preferring $GABA_A$ ligands may be reduced.

Abbreviations: ACSF, artificial CSF; BIC, bicuculline; CaMKII, Ca^{2+}/Calmodulin-dependent protein kinase II; CP, capacitance; DGGC, dentate gyrus granule cell; DS2, 4-chloro-N-[2-(2-thienyl) imidazo[1,2a]pyridine-3-yl]benzamide; EDTA, 2,2′,2″,2‴-(Ethane-1,2-diyldinitrilo)tetraacetic acid; EGTA, Ethylene glycol-bis(2-aminoethylether)-N,N,N′,N′-tetraacetic acid; FLIPR, fluorescent imaging plate reader; FMP, FLIPR membrane potential; GBZ, gabazine; ICS, intracellular solution; IPSC, inhibitory post-synaptic current; NMDG, N-Methyl D-Glucamine; PTX, picrotoxin; RS, series resistance; RT, room temperature; SEM, standard error of mean; SNP, single nucleotide polymorphism; TCD, tonic current density; TEA, tetraethylammonium; Thio-THIP, 4,5,6,7-Tetrahydroisothiazolo[5,4-c]pyridin-3-ol; THIP, 4,5,6,7-Tetrahydroisoxazolo[5,4-c]pyridin-3-ol; TPMPA, (1,2,5,6-Tetrahydropyridin-4-yl)methylphosphinic acid; TTX, tetrodotoxin.

1 | INTRODUCTION

The functional $GABA_A$ receptor that comprises the orthosteric binding site for GABA is a pentamer typically composed of two α-, two β- and one γ- or δ-subunit. Sampled from a population of six α (1–6), three β (1–3), two γ (1–2) and one δ, the possible number of permutations is in the hundreds. However, assembly rules favouring distinct combinations allow for only a subset to exist in vivo (Martenson, Yamasaki, Chaudhury, Albrecht, & Tomita, 2017; Olsen & Sieghart, 2008). The anatomical localization is subunit-specific: Typically, the γ-subunit-containing receptors mediate a synaptic, fast inhibitory post-synaptic current (IPSC) and the δ- and the α_{4-6}-subunit-containing receptors mediate a slow extrasynaptic tonic current (Chandra et al., 2006; Farrant & Nusser, 2005). The magnitude of the tonic current is region- and neuron-specific.The general view is that GABA diffusing from synapses or released into extrasynaptic areas and buffered by GABA uptake is the main determinant of GABA in the CSF and of the tonic current (reviewed by Glykys & Mody, 2007; Lee & Maguire, 2014; Overstreet-Wadiche & McBain, 2015). However, several $GABA_A$ receptor subtypes in recombinant systems, cultured hippocampal neurons and acute slices also display a degree of constitutive activity (Birnir, Everitt, Lim, & Gage, 2000; Hoestgaard-Jensen et al., 2014; McCartney, Deeb, Henderson, & Hales, 2007; Othman et al., 2012; Tang, Hernandez, & Macdonald, 2010; Wlodarczyk et al., 2013). For example, the receptor subunit combinations $\alpha_{1/4}\beta_3\gamma_{2(L)}$ and $\alpha_4\beta_{1/3}\delta$ are capable of both GABA-activated and constitutive gating, the latter ($\alpha_4\beta_3\delta$) in a manner dependent on PKA activity (Hoestgaard-Jensen et al., 2014; Jensen et al., 2013; Tang et al., 2010). Since the hippocampal dentate gyrus granule cells (DGGCs) in adult rats and mice exhibit high levels of co-expressed α_4-, $\beta_{1/3}$- and δ-subunits (Sperk, Schwarzer, Tsunashima, Fuchs, & Sieghart, 1997), this suggests that $\alpha_4\beta_{1/3}\delta$ $GABA_A$ receptors are very probable inhabitants at peri- and extrasynaptic loci in DGGCs (Chandra et al., 2006; Herd et al., 2008; Wei, Zhang, Peng, Houser, & Mody, 2003; Zhang, Wei, Mody, & Houser, 2007). A valuable tool for discriminating $\alpha_4\beta\delta$ subtypes is the orthosteric agonist 4,5,6,7-tetrahydroisothiazolo[5,4-*c*]pyridin-3-ol (**Thio-THIP**), which is highly selective for $\beta_{1/3}$ over β_2-containing subtypes (Hoestgaard-Jensen et al., 2014). By contrast, the closely related compound **4,5,6,7-tetrahydroisoxazolo[5,4-c]pyridin-3-ol (THIP**) does not display this selectivity (used for reference in the present study). In a previous study, application of Thio-THIP, paradoxically suggested a very limited expression of $\alpha_4\beta_{1/3}\delta$ receptors in DGGCs and mainly at synaptic loci (Hoestgaard-Jensen et al., 2014). Because constitutively active receptor populations of the $\alpha_4\beta_3\delta$ subtype in recombinant systems simultaneously display reduced efficacy to low levels of GABA (Jensen et al., 2013; Tang et al., 2010), we hypothesize that the absent response to Thio-THIP in DGGCs could be due to the presence of a constitutive current, providing a so-called baseline-floor effect of tonic inhibition (Tang et al., 2010). For these reasons, the present study was designed to separate the constitutive and agonist-mediated gating in $\alpha_4\beta_{1/3}\delta$ receptors in DGGCs using a systematic approach of different recording conditions and a carefully selected set of pharmacological tool compounds (Thio-THIP and THIP), the neutral antagonist **gabazine** (GBZ), the inverse agonist **bicuculline** (BIC) and the channel blocker **picrotoxin** (PTX). Gabazine was previously shown to be inactive towards constitutively active receptors, that is, designated as a neutral antagonist. Thus, part of this work also sought to reassess the precise pharmacological action of gabazine.

What is already known

- The $\alpha_4\beta_{1/3}\delta$ $GABA_A$ receptors exhibit both ligand-mediated and spontaneous gating.
- Spontaneous gating by $GABA_A$ receptor channels in neurons cannot be inhibited by gabazine.

What this study adds

- The spontaneous gating by $GABA_A$ receptors in hippocampal granule cells is kinase-dependent.
- Efficacy of $GABA_A$ orthosteric agonists at δ-subunit-containing receptors depend on the level of constitutive activity.

What is the clinical significance

- The agonist efficacy at $\alpha_4\beta_{1/3}\delta$ receptors in vivo is dependent on the intracellular kinase activity.
- This is relevant to pathologies such as addiction and epilepsy.

2 | METHODS

2.1 | Chemical compounds

THIP and Thio-THIP were synthesized at the Department of Drug Design and Pharmacology, University of Copenhagen, as previously described (Krehan et al., 2003). **CGP54626**, **tetrodotoxin (TTX)**, gabazine, **(1,2,5,6-Tetrahydropyridin-4-yl)methylphosphinic acid (TPMPA)**, PKC autoinhibitory peptide (19–36), **(4-chloro-N-[2-(2-thienyl)imidazo[1,2a]pyridine-3-yl]benzamide (DS2)** and GABA were obtained from Tocris Bioscience (Bristol, UK), while **kynurenate**, **strychnine, atropine**, picrotoxin and bicuculline-methiodide were obtained from Sigma-Aldrich (St. Louis, MO, USA).

2.2 | Animal work and compliance with requirements for studies using animals in accordance with ARRIVE

Animal studies are reported in compliance with the ARRIVE guidelines (Kilkenny, Browne, Cuthill, Emerson, & Altman, 2010) and with the recommendations made by the *British Journal of Pharmacology*. The use of rat and mouse tissue for the present studies were necessary because the specific receptor pharmacology under study is dependent on neuron-specific receptor-interacting kinases and furthermore requires a functional synaptic circuitry, none of which can be faithfully reproduced in recombinant systems. All use and housing of animals described below were carried out in accordance with the European Communities Council Directive (86/609/EEC) for the care and use of laboratory animals and the Danish legislation regulating animal experiments. Adult male Sprague Dawley rats were obtained from Envigo and housed socially in cages holding up to six rats with ad libitum access to food and water in rooms maintained at 22–24°C, 55% humidity at a 12-h/12-h normal night/day cycle. Rats were housed for 7–21 days and aged 49–70 days at the time of experiment (weighing 230–300 g). Mice strains (described below) were bred at in-house facilities and housed socially as described for rats. Only male mice at the age range of 60–120 days (weighing 25–35 g) were used. Cages were equipped with standard woodchip bedding, wood gnawing blocks, nestlets, cardboard tunnels (mice only) and red plastic huts. On the day of experiment, animals were terminated by decapitation (rats) or cervical dislocation (mice).

For mouse studies, δ and β_1 $GABA_A$ receptor subunit null (germline) mutants were employed. A breeding pair of mice heterozygous for the δ deletion (Mihalek et al., 1999) of the strain C57BL/6J × 129Sv/SvJ was kindly provided by Dr. Delia Belelli, University of Dundee, Scotland and bred in-house. Mice carrying deletions in the β_1 gene were generated and bred in-house as described below. All mice were bred at the specific pathogen-free animal facility at the University of Copenhagen. For both δ and β_1 deleted strains, heterozygotes were intercrossed to create littermates of all three genotypes ($^{-/-}$, $^{+/+}$ and $^{+/-}$) and monitored by PCR genotyping. Only $^{-/-}$ and $^{+/+}$ male mice resulting from heterozygous breeding were used for the studies.

2.3 | Production of $\beta_1^{-/-}$ mice

For the generation of mice with a targeted deletion of *gabrb1*, a Knockout First promoter driven mouse Gabrb1tm1a(KOMP)Wtsi was purchased from the KOMP repository (www.komp.org) and used to generate a full germline knockout ($\beta_1^{-/-}$). In the current study, only constitutive knockout mice were used. The conditional strain was simply a necessary intermediate step in the process of generating the full knockout. To this end, the obtained mouse was first crossed with a global Flp-expressing mouse to generate a conditional *loxP*-flanked (floxed) allele. Secondly, this mouse was crossed with a global Cre-expressing mouse to generate mice with a constitutive knockout allele, $\beta_1^{+/-Cre+}$. These were back-crossed into the C57BL/6 background to remove the *Cre* and *Flp* and to produce a genetically pure offspring and carefully monitored by PCR analysis. The resulting mouse lacks exon 4 of the *gabrb1* gene and instead contains one *frt* and one *loxP* site. After several steps of backcrossing to the C57BL/6J background strain, the generation equivalent level was determined by speed congenics using single nucleotide polymorphism (SNP) analysis technology (1450 SNP marker panel) (Taconic, Lille Skensved, Denmark). Of seven tested heterozygous males, all were found to be at least 99.72% identical to the C57BL/6J background, thus at least equivalent to the N8 generation. The resulting knockout, mice lacking either one or both deleted alleles ($\beta_1^{+/-}$ or $\beta_1^{-/-}$), was viable and born at expected Mendelian ratios. The mice were normal in their development, fertile and did not exhibit obvious behavioural or physical phenotypes. Animals were genotyped using the REDExtract-N-Amp™ Tissue PCR Kit (Sigma-Aldrich) according to the manufacturer's instructions. Primers were designed to discriminate knockout and wild-type β_1 alleles (forward primer 5′-GTATGGTCAGATGTCCTCAC-3′ and reverse primer 5′-CTGTCTTGCTAGCTTTGAG-3′). The amplification was as follows (94°C 5 min initial; then 94°C 30 s, annealing at 57°C for 30 s, extension at 72°C for 1.5 min for 35 cycles) to generate fragments of 1,211 bp for wild-type allele and 572 bp for the knockout allele. All mice used were genotyped before experiments. Expression at the protein level was also assessed with Western blot (see below).

2.4 | Slice electrophysiology

At the day of experiment, a single rat or mouse was decapitated and the head immediately immersed in ice-cold artificial CSF (ACSF, composition below) for 6–8 min before dissection of the brain. For dissection and slicing of the brain, ACSF contained (in mM): N-Methyl D-Glucamine (NMDG, 100), NaCl (26), KCl (2.5), $CaCl_2$ (1), $MgCl_2$ (3), $NaHCO_3$ (26), NaH_2PO_4 (1.25), D-glucose (10), ascorbate (0.3), pyruvic acid (0.3) and kynurenic acid (1), adjusted to 305 ± 3 mOsm and aerated with carbogen (95% O_2/5% CO_2). The brain was glued to the base of a Leica VT1200 S vibratome and cut in 350-μm-thick horizontal sections. Slices were stored at 28–29°C in a carbogenated ACSF of composition as above but without kynurenate and NMDG replaced with equimolar NaCl. Whole-cell patch clamp recordings of individual neurons in slices began after a 90-min recovery period and slices were used up to 4 h thereafter. Recording ACSF were in composition of bulk chemicals similar to storage ACSF but contained in addition kynurenate (1 mM), CGP54626 (1 μM), atropine (1 μM), strychnine (1 μM) and TTX (0.5 μM). During recordings, slices were maintained in a chamber holding 2 ml of ACSF at a flow rate of 2.8–3.0 ml·min^{-1} at a temperature of 23–24°C or 33–34°C. We used four different conditions for recording of the pharmacological effects of drugs efficacious at neuronal $GABA_A$ receptors, which we refer to as conditions *a*, *b*, *c* and *d*. For condition *a*, recordings were made at 23–24°C using an intracellular solution (ICS) composed of (in mM) CsCl (135), NaCl (4), $MgCl_2$ (2), HEPES (10), Ethylene glycol-bis(2-aminoethylether)-*N*,*N*,*N*′,*N*′-tetraacetic acid (EGTA, 0.05),

QX-314 (5), tetraethylammonium chloride (TEA, 5), Mg-ATP (2) and Na_2-GTP (0.5). The pH of the intracellular solution was adjusted to 7.2 with CsOH and held an osmolarity of 290–295 mOsm. For condition *b*, recordings were made at 33–34°C using the same intracellular solution. For condition *c*, recordings were made at 33–34°C, using the same intracellular solution but including 10 μM of the auto-inhibitory fragment (19–36) of PKC. For these experiments, an aliquot of the kinase inhibitor peptide was added to a prefiltered (0.22 μm) vial of intracellular solution before use. Condition *d* was performed also at 33–34°C, using intracellular solution of similar composition as in condition *b*, but in which the concentration of EGTA was increased from 0.05 to 10 mM and CsCl accordingly decreased to maintain osmolarity. Individual neurons were visualized in an IR video-microscope and recorded using thin-walled borosilicate pipettes (Sutter, outer/inner diameter 1.5/1.1 mm) with a 6- to 8-MΩ resistance (conditions *a*–*d*). To ensure a good diffusion of the intracellular solution into the neuron, we used an 8- to 9-min period between establishing the whole-cell configuration and beginning recording of baseline activity. Recordings of phasic and compound induced currents consisted of a 3-min baseline period, followed by a 6-min drug period (Thio-THIP, THIP and gabazine) and 3–5 min of bicuculline, gabazine or picrotoxin. Cell capacitance (CP) and series resistance (RS) were measured every 3–4 min throughout the recording and 80% compensated for series resistance. Cells were excluded from analysis if values for capacitance and series resistance deviated more than 30% from initial values determined at baseline. Whole-cell recordings were made using a Multiclamp 700A patch clamp amplifier controlled by pClamp 9 software and digitized at 10 kHz with a digidata 1322 (all Molecular Devices) and filtered (8-pole Bessell) at 3 kHz.

2.5 | Analysis of patch clamp recordings in dentate gyrus granule cells (DGGCs)

The average holding current value was assessed as the centre value, xc, of a single Gaussian fit of the general expression $A * e^{-0,5 * \left(\frac{x-xc}{w}\right)^2}$ to single-point trace values in a 2-min period (1 min for final antagonist) sampled at a 100 -ms interval. The analysis window for baseline and drug periods ended immediately prior to beginning of bath perfusion of the ensuing drug. The tonic current density (TCD) was calculated as the difference in holding currents divided by the cell capacitance ($pA{\cdot}pF^{-1}$) and all tonic current density D values are reported ± SD. Thus, an increase in the $GABA_A$ receptor gating (e.g. by an agonist) results in a negative value for tonic current density. A positive value for tonic current density occurs when the current shuts. The noise was analysed in some cases and was calculated as the centre value of a Gaussian fit to values of SD of 2-ms periods sampled at 100-ms intervals. Endogenous tonic and compound induced currents, noise analysis and evoked events were analysed in Clampfit 9 and Origin (OriginLab, 2017). Miniature inhibitory post-synaptic currents (mIPSCs) were analysed in Synaptosoft (6.07) and Origin as previously detailed (Hoestgaard-Jensen et al., 2014). Synaptic events included in the average waveform were detected when exceeding a threshold 6* the signal SD (unit pA), determined in the drug period to obviate false detections due to the increased noise during Thio-THIP application. The noise was also measured as the trace SD. The EC_{50} value for gabazine was determined as the concentration of half-maximal effect (x_0) in a fit to a logistic function of the general expression $= \left(\frac{A1-A2}{1+\left(\frac{x}{x0}\right)^p}\right)$.

2.6 | Whole-cell patch clamp electrophysiology on recombinant HEK-293 cells

Whole-cell patch clamp electrophysiology was performed on recombinant α4β1δ receptors expressed in HEK-293 Flp-In cells stably expressing the human $GABA_A$ δ-subunit (Falk-Petersen et al., 2017); 48 h before performing, the assay cells were transfected using the polyfect transfections reagent (as described for the FLIPR membrane potential [FMP] assay) with a 1:1 ratio of human α_4 (pUNIV plasmid) and human β_1 (pUNIV plasmid) co-transfected with GFP (1.4 mg + 1.4 mg + 1.2 mg) for positive selection of transfected cells. The day before, assay cell were seeded on PDL coated coverslips and on the day of the assay transferred to a chamber placed on the stage of an Axiovert 10 microscope (Zeiss, Germany), containing artificial balanced salt solution (ABBS) with the following composition (in mM): NaCl 140, KCl 3.5, Na_2HPO_4 1.25, $MgSO_4$ 2, $CaCl_2$ 2, glucose 10 and HEPES 10; pH 7.35. The temperature was controlled by a TC-344C temperature controller with a SH-27B solution in-line heater (Warner Instruments, USA) to 33–34°C measured in the chamber.

The cells were approached with micropipettes of 2.1- to 3.2-MΩ resistance manufactured from 1.5 mm OD glass (World Precision Instruments, Sarasota, Florida) on a microelectrode puller, model PP-830 (Narishige, Tokyo, Japan). The intrapipette solution resembled conditions *b* and *d* contained the following (in mM): CsCl (130 or 140), NaCl (4), $MgCl_2$ (2), EGTA (10 or 0.05), MgATP (2), Na_2-GTP (0.5) and HEPES (10); pH 7.3. Cells were viewed at 200× magnification and cells containing GFP were visualized with UV light from an HBO 50 lamp (Zeiss, Germany). Recordings were made using the standard patch-clamp techniques in the whole-cell configuration and in voltage clamp mode, filtered (4-pole Bessel) at 3 kHz and digitized at 10 kHz using an EPC-9 amplifier controlled by Pulse Software (HEKA, Germany). A clamping potential of −60 mV was used, series resistance was 80% compensate and compounds were bath applied for 15 s with an application flow of 2 $ml{\cdot}min^{-1}$. Data were analysed in IgorPro version 6.22A (HEKA, Germany).

2.7 | $GABA_A$ receptor expression and FLIPR™ membrane potential Blue Assay on HEK-293 cells

The FMP assay was performed on HEK-293 Flp-In™ cells expressing the human $\alpha_4\beta_1\delta$ and $\alpha_4\beta_3\delta$ $GABA_A$ receptor as described previously (Falk-Petersen et al., 2017). In brief, HEK-293 Flp-In cells stably expressing the human $GABA_A$ δ-subunit (HEK-δ cells) were transfected in a 1:1 ratio (4 μg + 4 μg) of human α_4 (pUNIV plasmid) and

human β_1 (pUNIV plasmid) and 2:0.01 ratio (8 μg + 0.04 μg) of α_4 to human β_3 (pcDNA3.1) using Polyfect Transfection Reagent (Qiagen, West Sussex, UK). The latter ratio was optimized in a previous study to limit the formation of β_3 homomers (Falk-Petersen et al., 2017); 16–24 h after transfection, cells were plated into black poly-D-lysine coated clear bottom 96-well plates (BD Biosciences, Bedford, MA, USA) at 50,000 cells per well. After 16–20 h, the media was aspirated, cells were washed in assay buffer and added 100 μl per well of FMP blue dye (0.5 mg·ml^{-1}) (Molecular Devices) (Sunnyvale, CA, USA) followed by incubation for 30 min in a humidified 5% CO_2 incubator at 37°C. Compound solutions were prepared in assay buffer in 5× which for antagonist testing contained a concentration of GABA corresponding to GABA EC_{80}. Compounds were added to a 96-well ligand plate and incubated for 15 min at the desired recording temperature (either 25°C or 37°C) in the NOVOstar™ plate reader (BMG, LABTECH GmbH, Offenburg, Germany). The plate was read using an emission wavelength of 560 nm caused by excitation at 530 nm with the response detected as changes in fluorescent signal given in fluorescent units (ΔFU). The obtained data are based on five experiments from separate batches of transfected cells, each with three technical replicates. All potency determinations were based on at least five independent experiments and data from inactive compounds on five independent experiments. Data were analysed as relative changes in the fluorescent signal by taking the maximum compound induced peak/plateau signal and subtracting the baseline signal. Changes in the fluorescent signal caused by compound addition to the wells and artefacts were manually omitted from the analysis. Concentration–response curves were fitted using the four-parameter concentration–response curve:

$$Response = bottom + \frac{top - bottom}{1 + 10^{((log(EC_{50}) - [A]) \cdot n_H)}}$$

with bottom being the lower plateau response and top the upper. [A] is the logarithmic concentration of the compound and n_H the hill slope. Antagonists were fitted using the same equation giving IC_{50} instead of EC_{50} as for the agonist.

2.8 | Western blots

After decapitation, the cortex was rapidly dissected out from at least four $\beta_1^{+/+}$ or $\beta_1^{-/-}$ mice and tissues individually snap-frozen on dry ice and stored at −80°C until use. Crude membranes were prepared from each sample by quickly thawing the brain tissue at 37°C and adding 5× *w*/*v* of 50-mM Tris HCl, pH 7.4 supplemented with 2,2′,2″,2‴-(Ethane-1,2-diyldinitrilo)tetraacetic acid (EDTA)-free protease inhibitors (Roche). Tissue was homogenized using 2 × 1 mm zirkonium-oxide beads using a Bullet Blender (Next Advance, NY, USA) for 30 s at max. speed. The protein concentration was determined using Bradford protein assay and 10 μg of each sample was added sample buffer and reduced using 100-μM dithiotreitol and incubated for 15 min at 40°C and 15-s sonication before loading onto a Mini-Protean TGX gel (4%–20%, BioRad) and run for 40 min at 200 V. Protein gels were blotted onto PVDF membranes using the Trans-Blot Turbo Transfer System (BioRad). Following blocking in 3% BSA in 1× Tris buffered saline-Tween20 buffer for 60 min at room temperature (RT), blots were probed overnight at 4°C with anti-β_1 (gift from the Medical University of Vienna, Center for Brain Research). The antibody was raised against an epitope (350–408) of the mouse β_1 protein and used at a concentration of 0.5 μg·ml^{-1}. Primary antibodies were detected with HRP-conjugated goat anti-rabbit antibody (#PI-1000, RRID:AB_2336198, Vector Laboratories, USA) and visualized by chemiluminescence (Amersham ECL Prime (GE Healthcare Biosciences, Pittsburg, PA, USA) using FluorChem HD2 (Alpha Innotech, San Leandro, CA, USA). Protein levels were visualized using Image Studio Lite Ver 5.2. The immuno-related procedures used comply with the recommendations made by the *British Journal of Pharmacology* (Alexander et al., 2018).

2.9 | Experimental design and statistical analysis

The data and statistical analysis comply with the recommendations of the *British Journal of Pharmacology* on experimental design and analysis in pharmacology (Curtis et al., 2018). The experiments were designed to use groups of equal size, with the size depending on the type of experiment based on experience and reproducibility of the assays. In general, a group size of n = 10–15 was used for slice and patch-clamp experiments and $n \geq 5$ for FMP experiments, based on obtaining standard error of mean (SEM) values on the pooled EC/IC_{50} values < 0.2. The exact group sizes used in the experiments are given in figure legends and tables and stated in the text in Section 3 in connection to the relevant data and analysis. For all group sizes less than 5, data are stated as preliminary with the exact n stated in the text. All given ns represent biological replicates and are the ns used when performing statistical analysis.

Hypothesis testing was performed either using one-way ANOVA with Bonferroni post hoc test for multiple comparisons, or as Student's *t*-tests for either pair-wise or unpaired comparisons, depending upon the experimental design (specified in the figure legends) all with a threshold for statistical significance of $P < 0.05$ deemed before performing the analysis. In connection with each experiment, the statistical test employed along with the F value (when applicable), standard error and number of experiments are stated. Statistical tests were only performed for group sizes of n = 5 or more.

Data are stated as mean ± SD except for recombinant experiments in HEK-293 cells, in which mean potencies are stated as pEC_{50}/pIC_{50} ± SEM. All concentration–response curves are presented using log-transformed concentrations on the x-axis to obtain normal data and sigmoidal curves.

2.10 | Nomenclature of targets and ligands

Key protein targets and ligands in this article are hyperlinked to corresponding entries in http://www.guidetopharmacology.org, the

common portal for data from the IUPHAR/BPS Guide to PHARMACOLOGY (Harding et al., 2018) and are permanently archived in the Concise Guide to PHARMACOLOGY 2019/20 (Alexander et al., 2019).

3 | RESULTS

We set out to determine the magnitude of the constitutive and the agonist-induced current in dentate gyrus granule cell (DGGCs) in the presence of TTX under varying conditions of temperature, free intracellular Ca^{2+} concentration and PKC activity. We utilized four specific conditions, *a* (24°C and 50-μM EGTA in the intracellular solution), *b* (34°C and 50-μM EGTA in the intracellular solution), *c* (34°C including 10-μM PKC 19–36 autoinhibitory peptide and 50-μM EGTA in the intracellular solution) and *d* (34°C and 10-mM EGTA in the intracellular solution) which aresummarized in Figure 1. We found that the magnitude of the endogenous tonic current after blocking $GABA_A$ receptors with 20-μM bicuculline was significantly larger in recording condition *b*, compared to conditions *a*, *c* and *d* with no difference between *a*, *c* and *d* (Figure 1a; Table 1). We also assessed the bicuculline sensitive tonic current density in $\delta^{-/-}$ mice by recordings made in conditions *b* and *d* (Figure 1c). In recording condition *b*, a tonic current density mean of 0.7 ± 0.3 was measured in $\delta^{+/+}$ mice compared to 0.0 ± 0.4 in $\delta^{-/-}$ mice (n = 9/10). In recording condition *d*, the bicuculline-induced tonic current density was 0.0 ± 0.4 in $\delta^{+/+}$ and 0.1 ± 0.2 in $\delta^{-/-}$ mice (n = 10/11), indicating that the receptors responsible for the tonic current density in condition *d* are dependent on incorporation of the δ-subunit. Because network levels of extracellular GABA were unlikely to be influenced by the composition of the intracellular solution in a single neuron, it appears plausible that the tonic current density in condition *b* (Figure 1a, b) is a result of predominantly constitutively active receptors, consistent with the idea that bicuculline is an inverse agonist (Birnir et al., 2000). It is important to stress that the absence of an endogenous tonic current in condition *a*, *c* and *d* in Figure 1a and throughout all experiments is due to the presence of TTX and the absence of exogenously added GABA in the ACSF (see Lee & Maguire, 2014, for review). Generally, for the measurement of the constitutive current, endogenous GABA inducing a tonus is a confounder, which is necessary to minimize.

To proceed, two cases were considered: If extracellular levels of GABA mediated the tonic current density in condition *b*, $GABA_A$ receptors could be internalized in conditions *a*, *c* and *d*, thus not in the capacity to respond to the extracellular levels of GABA. If, on the other hand, the tonic current density in condition *b* was due to constitutive activity, then channels must be either shut or internalized in conditions *a*, *c* and *d*. In either case, the effect of bath-applied orthosteric agonists should reveal if the recording conditions had created a functional difference in the number of receptors available for activation. We therefore tested the δ-subunit selective agonists Thio-THIP (100 μM) and THIP (2 μM) in conditions *a* through *d* (Figure 2). In order to compare with effects of gabazine (below), for these and the

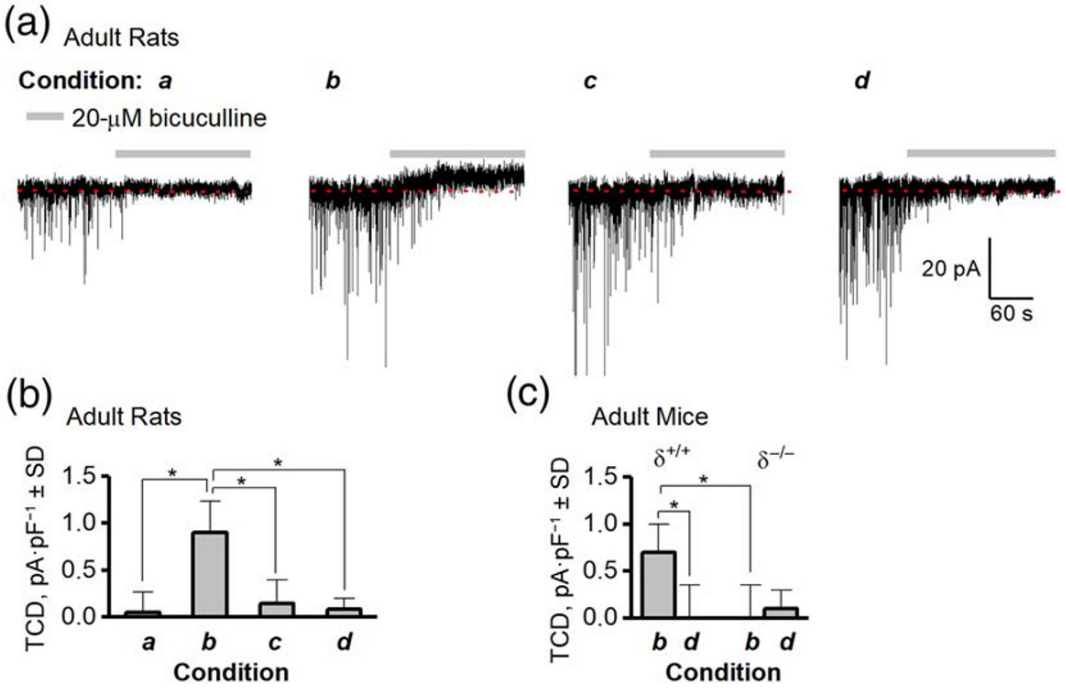

FIGURE 1 The magnitude of the $GABA_A$ receptor TCD in adult rat and mouse dentate gyrus granule cells (DGGCs) depend on recording condition and expression of the δ-subunit. The four recording conditions were *a*: 24°C and 50-μM EGTA in the intracellular solution (ICS), *b*: 34°C and 50-μM EGTA in the intracellular solution (ICS), *c*: 34°C including 10-μM PKC 19–36 autoinhibitory peptide and 50 μM EGTA in the ICS and *d*: 34°C and 10-mM EGTA in the ICS. (a) Representative recording traces showing that 20-μM bicuculline (BIC) blocks IPSCs under all recording conditions but also blocks a tonic current in condition *b*, which is absent in condition *a*, *c* and *d*. (b) Summary of data from (a); see also Table 1. (c) Summary of TCD in DGGCs recorded in condition *b* in $\delta^{+/+}$ and $\delta^{-/-}$ mice (n = 10 and 11, respectively). *P < 0.05, ANOVA/Bonferroni

TABLE 1 Summary of the effect of bicuculline (BIC), Thio-THIP, THIP and gabazine (GBZ) on the TCD in adult male rat dentate gyrus granule cells (DGGCs) recorded under four different conditions (*a*–*d*)

	Condition *a*	Condition *b*	Condition *c*	Condition *d*
	24°C	34°C	34°C, 50-μM EGTA	34°C
Temperature and ICS	50-μM EGTA	50-μM EGTA	10-μM PKC inh.	10-mM EGTA
Drug	TCD, $pA \cdot pF^{-1}$ ± SD (no of cells)			
20-μM BIC (Figure 1)	0.0 ± 0.2 (12)	0.7 ± 0.2* (13)	0.1 ± 0.4 (14)	0.1 ± 0.3 (12)
100-μM Thio-THIP (Figure 2) + 100-μM PTX	−1.2 ± 0.4 (12) 0.1 ± 0.4	−0.3 ± 0.3* (14) 0.9 ± 0.3*	−1.1 ± 0.3 (14) 0.1 ± 0.4	−1.2 ± 0.2 (12) −0.0 ± 0.2
2-μM THIP (Figure 2) + 100-μM PTX	−4.4 ± 0.7 (8) 0.1 ± 0.3	−2.4 ± 0.7* (8) 0.8 ± 0.4*	−5.5 ± 1.0 (8) −0.1 ± 0.3	−4.9 ± 1.2 (10) 0.1 ± 0.5
10-μM X (Figure 3) + 100-μM PTX	−1.0 ± 0.3 (10) 0.0 ± 0.4	−0.2 ± 0.2* (12) 0.9 ± 0.3*	−1.1 ± 0.3 (12) 0.2 ± 0.3	−1.2 ± 0.3 (12) 0.2 ± 0.2

Note: Reported values are the tonic current density (TCD), calculated as the ratio of the difference in holding current between baseline and drug period over cell capacitance. Statistical difference is determined between compound effects in the different conditions by ANOVA followed by Bonferroni mean comparison. ICS, intracellular solution; PTX, picrotoxin.
*$P < 0.05$.

following experiments, we used picrotoxin rather than bicuculline to block agonist-induced currents.

These experiments revealed that the recording condition greatly influenced the magnitude of tonic current density induced by δ-subunit selective agonists in DGGCs. For 100-μM Thio-THIP, the tonic current density was significantly less in condition *b* compared to *a*, *c* and *d* (Figure 2 a, c,f–h, Table 1). Similarly to the effect of bicuculline, picrotoxin administered after Thio-THIP resulted in a tonic current density near 0 for conditions *a*, *c* and *d*, but 0.9 ± 0.3 for condition *b* (Table 1). The change in noise (only conditions *b* and *d* for Thio-THIP analysed) was not significant from baseline to Thio-THIP in recording condition *b* (mean pA ± SD) 1.61 ± 0.36 and 1.65 ± 0.39, respectively (n = 14), but was significantly increased in condition *d* from 1.72 ± 0.34 during baseline to 2.2 ± 0.4 in Thio-THIP (n = 12). We did not detect a difference in baseline noise in recording condition *b* vs. *d*. In a different set of experiments (cells not used for measurement of tonic current density), we calculated the reversal potential for the averaged mIPSCs in a 20-s window/step before and after Thio-THIP at incremental voltage shits (20 mV/step −70 to +30 mV and found a reversal of −2.2 ± 4.0 in control and 0.2 ± 4.2 mV in 100-μM Thio-THIP (not significant, n = 6). The tonic current density observed for THIP (2 μM, Figure 2f, g) displayed a similar recording condition-dependent effect as Thio-THIP, being nearly twice as large in conditions *a*, *c* and *d* compared to *b* (Table 1). Because of the significantly increased response to orthosteric agonists in conditions *a*, *c* and *d* vs. *b*, we conclude that a net receptor internalization could not be the reason for the absent constitutive current under conditions *a*, *c* and *d*. While the tonic current density induced by δ-subunit specific orthosteric agonists was highly dependent on recording condition (Figure 2a, c–g), the peak of the averaged non-contaminated mIPSC was, however, similarly diminished by Thio-THIP in all conditions (Figure 2b, d, e). For Thio-THIP (Figure 2d), the peak mIPSC was significantly reduced from (mean pA ± SD) −20.0 ± 6.3 to −15.8 ± 6.2 (condition; n = 12), in condition *b* from −35.6 ± 8.8 to −30.4 ± 9.0 (n = 14), in condition *c* from −38.7 ± 7.6 to −34.1 ± 7.6 (n = 14) and in condition *d* from −34.6 ± 8.7 to −29.1 ± 7.4 (n = 12). The mIPSC peak was significantly different in condition *a* to conditions *b*, *c* and *d*. The selectivity of Thio-THIP for δ-subunit-containing receptors in mediating effects on tonic current density and mIPSC peak was assessed in $\delta^{-/-}$ mice (Figure 2h). Recording from DGGCs in condition *d*, Thio-THIP (100 μM) induced a tonic current density of −0.8 ± 0.2, which significantly reverted to 0.2 ± 0.3 after picrotoxin in $\delta^{+/+}$ mice (n = 9), whereas the response to Thio-THIP in $\delta^{-/-}$ mice was −0.1 ± 0.2, which was not changed by picrotoxin (0.2 ± 0.2, n = 10). The response to Thio-THIP was significantly different between the two genotypes. Similarly, the Thio-THIP-induced reduction in mIPSC peak, observed in rat DGGCs (Figure 2b, d), was also seen in $\delta^{+/+}$ mice (−41.4 ± 9.0 pA in baseline vs. −37.4 ± 9.0 pA in Thio-THIP, n = 9), but absent in $\delta^{-/-}$ mice (−37.1 ± 7.6 in baseline vs. −37.2 ± 7.5 in Thio-THIP, n = 10).

It has been commonly observed that gabazine cannot close $GABA_A$ receptor channels displaying constitutive activity (McCartney et al., 2007; Wlodarczyk et al., 2013). However, the recognized ability to minimize the constitutive gating through the recording condition now offered a new and untried possibility for probing the antagonist effects of gabazine. If gabazine is a neutral antagonist at constitutively active receptors, it follows that we should expect a tonic current density near zero for gabazine in the conditions under which the constitutive gating is shut. However, in these conditions, gabazine (10 μM), although completely blocking all mIPSCs, also induced a tonic current density, that is, an apparent receptor activation in conditions *a*, *c* and *d* but not in condition *b* (see Table 1 for n in individual experiments). The block of the mIPSCs by gabazine was complete in <20 s from onset and coincident with onset of the tonic current density, which continued to develop for at least 2 min (Figure 3). A concentration–response relation of gabazine for this effect recorded in condition *d* gave an EC_{50} of 2.1 μM (five concentrations in the range 10-nM to 50-μM gabazine tested, Figure 3d, one concentration per cell). However, if the constitutive current in condition *b* was first shut by 20-μM bicuculline before

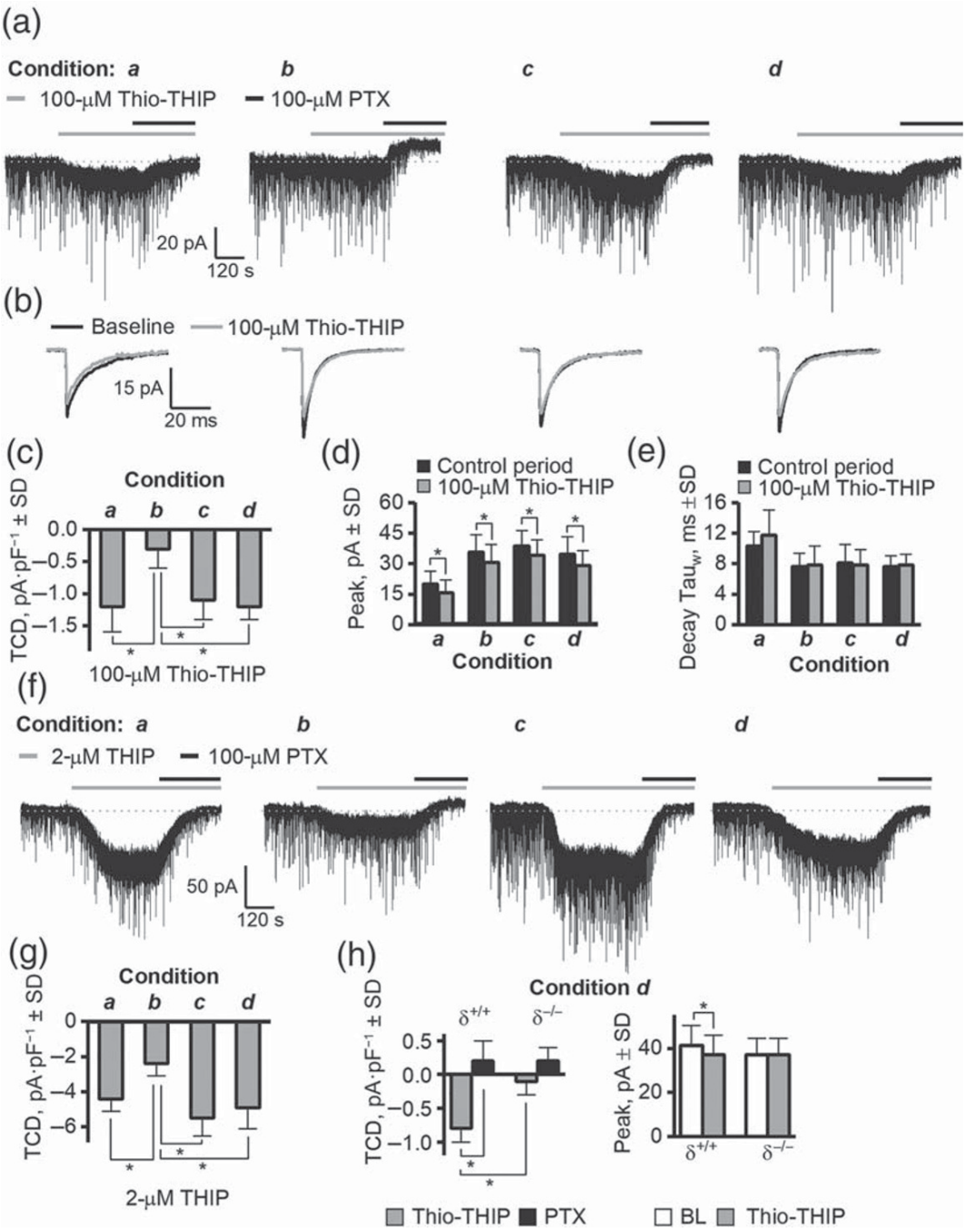

FIGURE 2 The effect of two GABA agonists, THIP (δ-subunit preferring) and Thio-THIP ($\alpha_4\beta_{1/3}\delta$ selective) on the TCD is dependent on temperature, intracellular Ca^{2+}-EGTA chelation and PKC activity. The four conditions *a*–*d* were *a*: 24°C and 50-μM EGTA in the intracellular solution (ICS), *b*: 34°C and 50-μM EGTA in the ICS, *c*: 34°C including 10-μM PKC 19–36 autoinhibitory peptide and 50-μM EGTA in the ICS and *d*: 34°C and 10-mM EGTA in the ICS. (a) Full recording traces of voltage clamped (−70 mV) DGGCs upon bath application of 100-μM Thio-THIP followed by picrotoxin (PTX). Thio-THIP induces an ∼4× larger TCD in conditions *a*, *c* and *d* than condition *b*. Note the presence of a positive endogenous TCD in condition *b* only. (b) Traces of mIPSCs display the Thio-THIP induced reduction of the average mIPSC in all recording conditions. (c) Summary barplot of TCD values induced by Thio-THIP (see Table 1 for individual *n*, **P* < 0.05 ANOVA/Bonferroni). (d,e) Summary of peak and decay time of the average mIPSCs (**P* < 0.05 paired *t*-test). (f,g) Representative traces and barplot showing the effect of THIP in recording conditions *a* through *d* (see Table 1 for individual *n*, **P* < 0.05 ANOVA/Bonferroni). (h) The TCD induced by Thio-THIP in adult $\delta^{+/+}$ and $\delta^{-/-}$ mice and the effect on the average mIPSC peak in the same recordings (*n* = 9 and 10, respectively, **P* < 0.05, paired Student's *t*-test for same-cell measurements, unpaired for different cells)

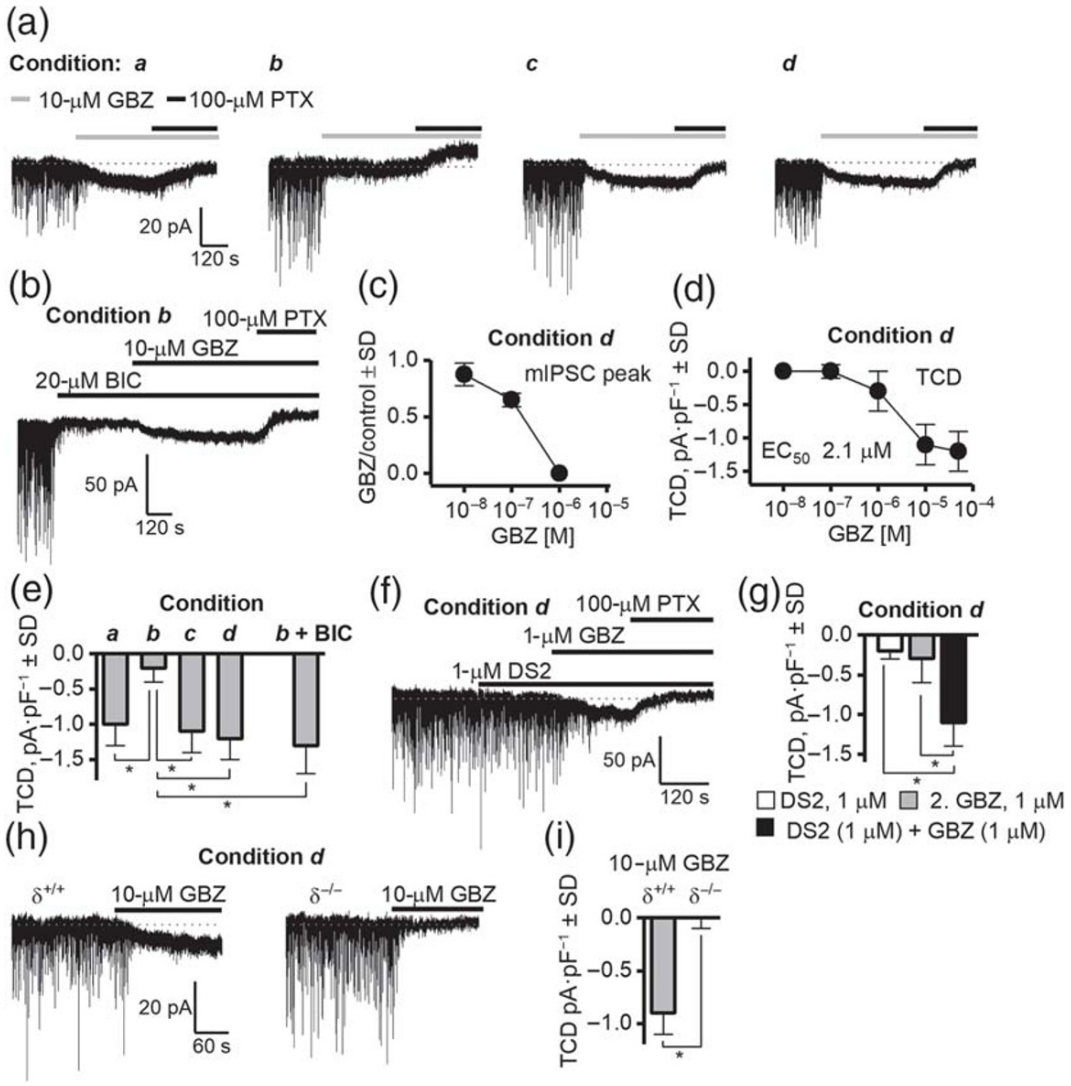

FIGURE 3 Gabazine (GBZ) induces a δ-subunit-dependent TCD in adult rat and mice dentate gyrus granule cells (DGGCs) under recording conditions phenomenologically characterized by the absence of a constitutive current. The four conditions *a*–*d* were *a*: 24°C and 50-μM EGTA in the intracellular solution (ICS), *b*: 34°C and 50-μM EGTA in the ICS, *c*: 34°C including 10-μM PKC 19–36 autoinhibitory peptide and 50-μM EGTA in the ICS, and *d*: 34°C and 10-mM EGTA in the ICS. (a) Recording traces displaying the effect of GBZ and picrotoxin (PTX) in recording conditions *a*–*d*. GBZ quickly blocks mIPSCs but also induces a TCD in conditions *a*, *c* and *d*, which is reversed by PTX. (b) Shutting of the constitutive current by bicuculline (BIC; 20 μM) in recording condition *b* is reversed by GBZ (10 μM). (c,d) Concentration–response relation of GBZ in blocking mIPSCs and inducing a TCD in recording condition *d*. (e) Summary of effects of GBZ to induce a TCD in recording conditions *a*–*d*, incl. recording condition *b* in which the constitutive current is shut by BIC. (f,g) The δ-subunit selective positive modulator DS2 potentiates the effect of GBZ in producing a PTX-sensitive current. (h,i) Recordings of DGGCs from adult $\delta^{+/+}$ and $\delta^{-/-}$ mice demonstrate that the effect of GBZ inducing a TCD is dependent on expression of the δ-subunit. For panel (i), $n = 7$ for each genotype $^*P < 0.05$, Student's *t*-test ANOVA/Bonferroni

perfusion of gabazine (10 μM), we found that gabazine now induced a tonic current density of −1.3 ± 0.4, which again could be shut by 100-μM picrotoxin (Figure 3b, as originally observed by Wlodarczyk et al., 2013). The difference in tonic current density produced by gabazine (10 μM) in condition *b* + 20-μM bicuculline and condition *c* or *d* (gabazine alone, from Table 1) was not significant.

To assess if this apparent agonistic effect of gabazine was dependent on $GABA_A$ receptors incorporating the δ-subunit, we first tested gabazine (1 μM) in the presence of the δ-subunit positive modulator DS2 (1 μM). In recording condition *d*, bath application of DS2 (1 μM) and subsequent (3 min later) administration of gabazine (1 μM) increased tonic current density to −1.1 ± 0.3 ($n = 8$). This was significantly larger than the tonic current density for application of 1-μM DS2 (−0.2 ± 0.1, $n = 5$) or 1-μM gabazine (−0.3 ± 0.5, $n = 8$) alone. Further, the effect of gabazine (10 μM) recorded under condition *d* in $\delta^{-/-}$ mice was 0.0 ± 0.1, but −0.9 ± 0.2 in $\delta^{+/+}$ mice (Figure 3i), indicating that the effects of gabazine in producing a tonic current density was indeed dependent on the presence of the δ-subunit. Finally, we assessed whether the effect of gabazine in producing a tonic current density could be mediated through homomeric **GABA receptor ρ1 subunit** and tested 10-μM TPMPA in condition *d*, which was ineffective in blocking the effects of gabazine. However, despite these clear effects of gabazine in inducing a current in

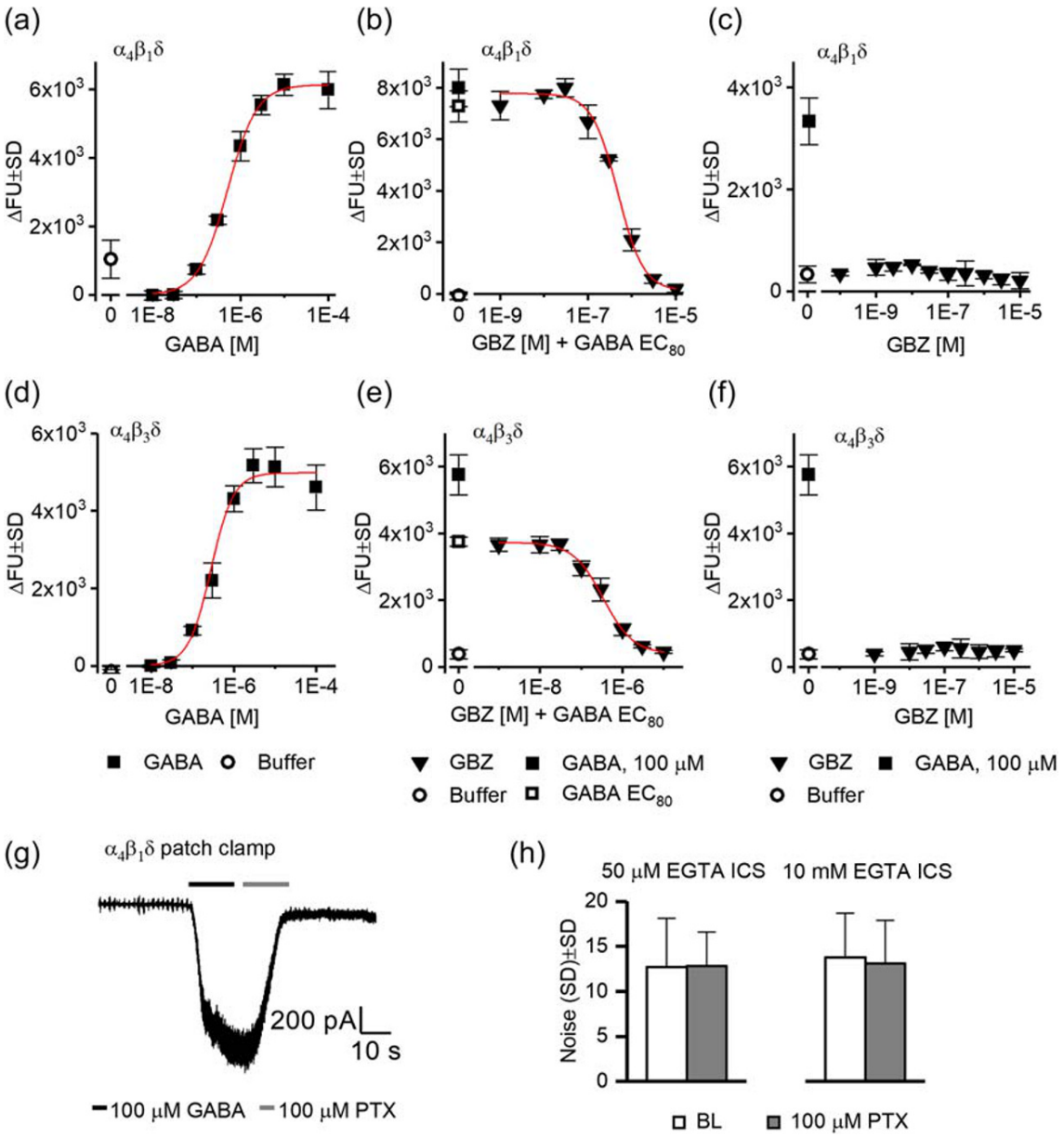

FIGURE 4 Gabazine (GBZ) antagonizes the effect of GABA but does not induce a current alone in constitutively silent $\alpha_4\beta_1\delta$ and $\alpha_4\beta_3\delta$ receptors expressed in HEK-293 Flp-In cells. (a,d) GABA (■) activates human $\alpha_4\beta_1\delta$ (a) and $\alpha_4\beta_3\delta$ (d) receptors with a similar EC_{50}s. (b,e) GBZ (▼) concentration-dependently blocks the response to an EC_{80} concentration of GABA with IC_{50} = 0.34 μM at $\alpha_4\beta_1\delta$ receptors (b) and 0.44 μM at $\alpha_4\beta_3\delta$ receptors (e). (c,f) GBZ does not induce a current alone in any receptor type. All datapoints in graphs (a–f) are means of triplicate measurements ± SD. FU, fluorescence unit. Symbols below both figures are the same in the three vertical panels. (g) Trace from a HEK-293 cell expressing $\alpha_4\beta_1\delta$ receptors and recorded from in patch clamp mode using an intracellular concentration of 50-μM EGTA, showing effect of GABA (100 μM) and PTX. (h) The noise values for baseline and PTX period in two different intracellular solutions (containing either 50-μM or 10-mM EGTA) which was not significantly different (Student's *t*-test), indicating no constitutive current

receptors incorporating the δ-subunit with at least partial contribution from the β_1-subunit (below, Figure 5), we could not demonstrate such effects of gabazine in HEK-293 cells expressing human recombinant $\alpha_4\beta_{1/3}\delta$ receptors (Figure 4). Using a recently characterized assay employing voltage-sensitive fluorescence emitting dyes (Falk-Petersen et al., 2017), the effect of GABA, gabazine and bicuculline was characterized at human $\alpha_4\beta_1\delta$ receptors at 37°C and 25°C. At 37°C, GABA displayed an EC_{50} value of 0.28 μM (pEC_{50} = 6.56 ± 0.10, *n* = 5) (Figure 4a) and gabazine displayed an IC_{50} value of 0.34 μM (pIC_{50} = 6.46 ± 0.14, *n* = 5) against a concentration of GABA EC_{80} (Figure 4b). Similarly, at human $\alpha_4\beta_3\delta$ receptors, GABA displayed an EC_{50} value of 0.36 μM (Figure 4d), and gabazine displayed an IC_{50} of 0.44 μM (Figure 4e). The constitutive activity at both 37°C and 22°C was negligible and we did not observe any current induced by gabazine at either receptor subtype (Figure 4c, f). We also tested if spontaneous currents were observed in $\alpha_4\beta_1\delta$ expressing HEK-293 cells recorded in regular whole-cell patch clamp electrophysiology at 34°C using intracellular solutions as used for condition *b* (*n* = 10) and *d* (*n* = 12) in slice experiments (Figure 4g, h).

GABA (100 μM) was applied for 15 s followed by 100 μM picrotoxin for 15 s. In each of these conditions, the noise at baseline was not significantly different from the noise in picrotoxin (for 50-μM EGTA intracellular solution, BL noise was 12.7 ± 5.4 vs. 12.8 ± 3.8 pA in PTX, for 10-mM EGTA intracellular solution, BL noise was 13.8 ± 4.9 vs. 13.1 ± 4.8 pA in PTX).

Because the effects of gabazine and Thio-THIP were both dependent on the presence of the δ-subunit and both ineffective at producing a significant tonic current density when the constitutive gating was present (condition *b*, Figure 2 and Table 1), we hypothesized that their effects were mediated by the same receptors. We tested in conditions *b* and *d* if gabazine (1 and 10 μM) could affect the tonic current density induced by Thio-THIP (100 μM). In condition *b*, Thio-THIP induced a tonic current density of −0.3 ± 0.3 which was not changed by 10-μM gabazine (Figure 5a). In condition *d*, the tonic current density induced by Thio-THIP (−1.2 ± 0.2, *n* = 13, Figure 5b) also was not significantly changed by 1-μM gabazine or 10-μM gabazine.

Because the effects of gabazine (at 10 μM, maximum effect, Figure 5b) and Thio-THIP were not additive, this suggested that their effects could be mediated through the same (saturable) mechanism. Thio-THIP displays a selectivity for the $\alpha_4\beta_{1/3}\delta$ receptor subtype, sparing other hippocampal δ-subunit partnerships. To assess if a β-subunit could be involved in this response, we repeated the Thio-THIP–gabazine interaction study in mice ablated of the β_1-subunit (Figure 5h) and made recordings in condition *d* (Figure 5c–g). In the $\beta_1^{+/+}$ mice (*n* = 18), Thio-THIP induced a tonic current density of −0.9 ± 0.3 compared to −0.7 ± 0.4 in $\beta_1^{-/-}$ mice. However, the ensuing effect of gabazine (10 μM) produced different effects on the tonic current density between genotypes. In $\beta_1^{+/+}$ mice, gabazine added after Thio-THIP produced a tonic current density of −0.9 ± 0.4 (Thio-THIP vs. Thio-THIP + gabazine, non-significant, Student's paired *t*-test, *n* = 18) but significantly reduced the tonic current density in $\beta_1^{-/-}$ mice to −0.4 ± 0.4 (Thio-THIP vs. Thio-THIP + gabazine, *n* = 22). The noise (SD) during baseline and during Thio-THIP application was independent on genotype (Figure 5e), whereas gabazine significantly reduced noise in $\beta_1^{-/-}$ to a level below that of the $\beta_1^{+/+}$ (gabazine + Thio-THIP in $\beta_1^{+/+}$ produced a noise of 1.37 ± 0.26 pA but 1.18 ± 0.29 pA in $\beta_1^{-/-}$ mice (*n* = 18 $\beta_1^{+/+}$ and 22 $\beta_1^{-/-}$). An additional qualitative observation was that the onset of the noise by Thio-THIP, or the shutting of it by gabazine, was fast (see Figure 5a, b, g), reaching a plateau within tens of seconds after onset, whereas the tonic current density by either Thio-THIP or gabazine continued to develop for typically 2 min after onset. These data obtained in $\beta_1^{-/-}$ mice infer that the gabazine response involves, at least in part, β_1-containing receptor subtypes—in addition to δ-subunit-containing receptors, possibly in a common subtype, for example, $\alpha_4\beta_1\delta$.

4 | DISCUSSION

In the present study, we show that the magnitude of the constitutive and the agonist-induced current passed by $\alpha_4\beta_{1/3}\delta$ $GABA_A$ receptors in adult rodent dentate gyrus granule cells (DGGCs) is determined by temperature, free intracellular Ca^{2+} levels and PKC activity. By comparing effects of the orthosteric agonists THIP and Thio-THIP, the orthosteric antagonists bicuculline and gabazine, and the channel blocker picrotoxin in four different recording conditions in adult rats, $\delta^{+/+}$, $\delta^{-/-}$, $\beta_1^{+/+}$ and $\beta_1^{-/-}$ mice, we demonstrate the existence of an inverse relationship of the constitutive versus the agonist-induced current in DGGCs. Further, we show that only under the conditions of a shut constitutive channel does gabazine induce a picrotoxin-sensitive current. This current is completely dependent on the expression and incorporation of the δ- and to some degree also the β_1-subunit in functional GABA receptors, elucidated with the first in vitro phenotypical description of a $\beta_1^{-/-}$ mouse strain. However, this effect of gabazine could not be replicated in human $\alpha_4\beta_{1/3}\delta$ receptors expressed in HEK-293 cells, suggesting a component missing in HEK cells, compared to DGGCs. Our data suggest that in vivo efficacy of δ-subunit preferring agonists (i.e. THIP) in DGGCs is diminished in conditions of increased PKC activity.

4.1 | Constitutive activity of $GABA_A$ receptors

The four different recording conditions (*a*: 24°C and low EGTA intracellular solution, *b*: 34°C and low EGTA intracellular solution, *c*: 34°C low EGTA including PKC inhibitor intracellular solution, and *d*: 34°C and high EGTA intracellular solution) were chosen because of previous findings that implicate temperature and kinase activity as regulators of δ-subunit-containing $GABA_A$ receptors (Bright et al., 2011; Bright & Smart, 2013; Houston, Lee, Hosie, Moss, & Smart, 2007; Wei et al., 2003). The results obtained from recording condition *b* (Table 1) compared to condition *c* or *d* suggest that the endogenous tonic current density is mediated by high intracellular kinase activity most likely mediating specific phosphorylation of receptor subunits (discussed below). Recordings at 24°C gave similar results as kinase inhibition at 34°C, which we suggest is a consequence of low kinase activity at 24°C, because PKC in this case does not readily translocate to the plasma membrane in mammalian cells (Chemin et al., 2007). Since the responses to the orthosteric agonists Thio-THIP and THIP were increased in conditions *a*, *c* and *d* relative to *b*, (Figure 2 and Table 1, see below), the same conditions for which the tonic current density was absent (*a*, *c* and *d*, Figure 1; Table 1), two conclusions are made. First, the absence of an endogenous tonic current density in conditions *a*, *c* and *d* is not due to internalization of δ-subunit-containing receptors and second, the tonic current density in condition *b* must be the result of constitutively active receptors that can be shut by PKC inhibition, bicuculline and picrotoxin (Figures 1 and 2; Table 1) but not by gabazine (see below). The constitutively active receptors recorded in condition *b* were also detected in $\delta^{+/+}$ but not in $\delta^{-/-}$ mice, identifying the δ-subunit as necessary and sufficient for the measured constitutive current.

4.2 | Response to THIP and Thio-THIP in different recording conditions

Results obtained with THIP and Thio-THIP were qualitatively similar. However, the ratio between tonic current density values obtained in conditions *c* and *b* (i.e. tonic current density(*c*)/tonic current density (*b*) ~ 2 for THIP but ~4 for Thio-THIP, calculated from the tonic current density values in Table 1) suggests that PKC inhibition or chelation of intracellular Ca^{2+} affect receptors that are targets for Thio-THIP more selectively. We shall therefore focus this discussion on $\alpha_4\beta_{1/3}\delta$ receptors due to the selectivity of Thio-THIP for these (Hoestgaard-Jensen et al., 2014). Since the $\alpha_4\beta_{1/3}\delta$ receptors, but not

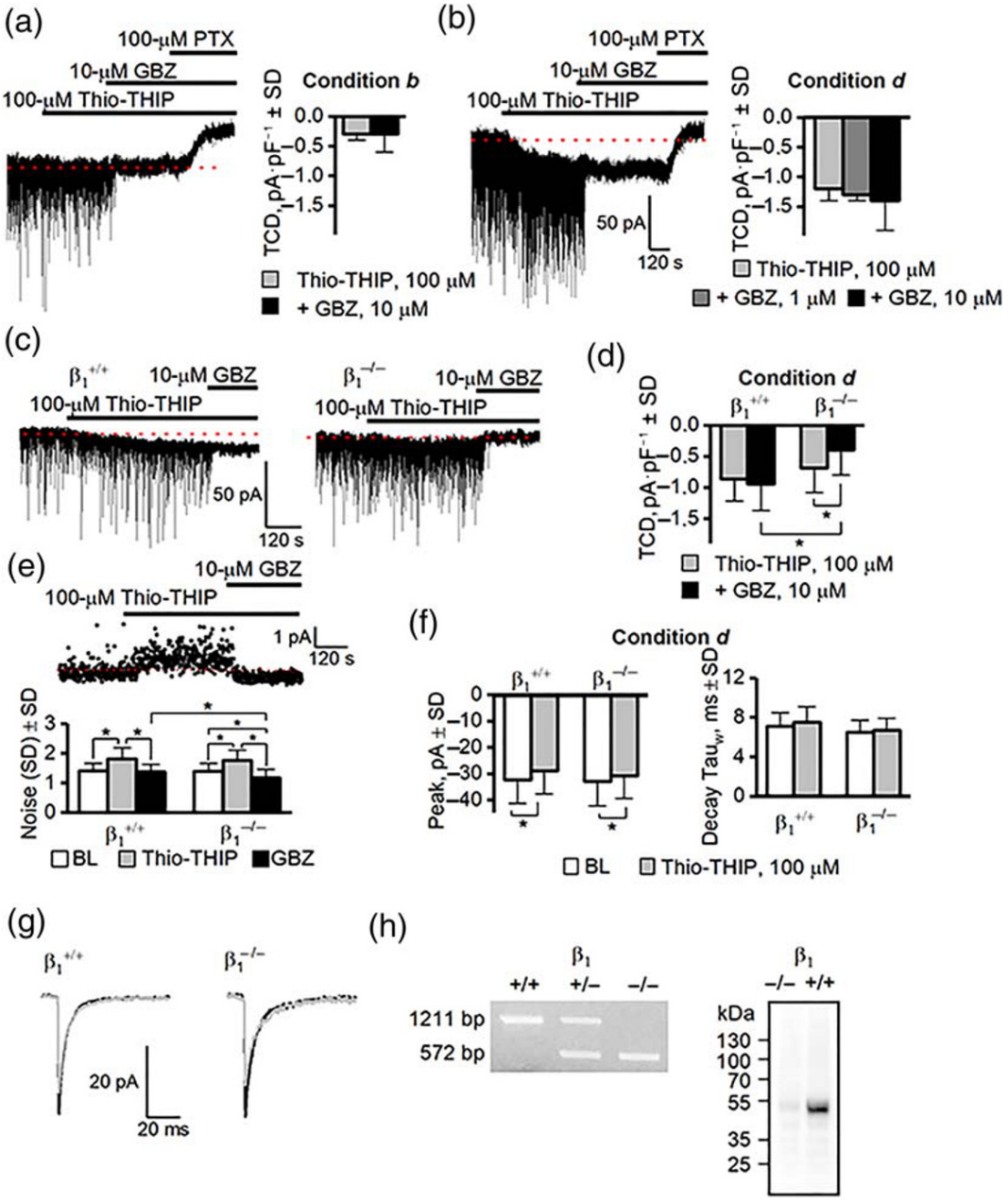

FIGURE 5 Gabazine (GBZ) does not antagonize the effect of Thio-THIP. Recording conditions used here were *b*: 34°C and 50-μM EGTA in the intracellular solution (ICS) and *d*: 34°C and 10-mM EGTA in the intracellular solution (ICS). (a) Thio-THIP, GBZ and picrotoxin (PTX) on DGGCs in recording condition *b* in adult rats (*n* = 8). (b) Same experiment as (a), recording condition *d*. Note that 10-μM GBZ neither blocks nor increases the TCD already induced by Thio-THIP (right panel, *n* = 13). (c,d) Thio-THIP and GBZ recorded in condition *d* in adult $\beta_1^{+/+}$ and $\beta_1^{-/-}$ mice (*n* = 18 and 22, respectively). (e) The noise (SD) induced by Thio-THIP and GBZ in $\beta_1^{+/+}$ and $\beta_1^{-/-}$ mice. The noise in Thio-THIP + GBZ is significantly lower in $\beta_1^{-/-}$ than $\beta_1^{+/+}$ mice. (f,g) The average mIPSC peak is similarly reduced by Thio-THIP in $\beta_1^{+/+}$ and $\beta_1^{-/-}$ mice. (h) Left: Representative example of PCR genotyping of samples from $\beta_1^{+/+}$, $\beta_1^{+/-}$ and $\beta_1^{-/-}$ mice. Right: Representative preliminary Western blot of $GABA_A$ β_1-subunit in cortical brain homogenate from $\beta_1^{+/+}$ and $\beta_1^{-/-}$ mice showing absence of β_1-subunit immunoreactivity in $\beta_1^{-/-}$ mice ($\beta_1^{-/-}$, *n* = 4, $\beta_1^{+/+}$, *n* = 5)

$\alpha_4\beta_2\delta$ receptors, exhibit constitutive gating in oocytes and upon PKA-activation in HEK cells (Hoestgaard-Jensen et al., 2014; Jensen et al., 2013; Tang et al., 2010), these subtypes appear plausible candidates or the constitutive gating in DGGCs. Studies examining the co-existence of a PKA-activated constitutive current and a GABA-activated current in $\alpha_4\beta_3\delta$ $GABA_A$ receptors in HEK cells demonstrated that the constitutive current sets the baseline floor, under which sufficiently low concentrations of agonist are ineffective in increasing channel open probability (Tang et al., 2010). Our data in DGGCs are in support of this, since the effect of Thio-THIP on the tonic current density is minimal in condition *b* (high constitutive current), but ~4 times more effective in conditions *a*, *c* and *d* (no constitutive current, Figures 1a and 2a).

The effect of a high concentration of EGTA or inhibitor of PKC in the intracellular solution on the endogenous tonic current density and response to agonists suggests an already high level of endogenous kinase activity and receptor phosphorylation at 34°C in the low concentration of EGTA in the intracellular solution (see also Brandon et al., 2000; Bright et al., 2011; Bright & Smart, 2013). It is therefore interesting to note that the effect of Thio-THIP on the synaptic response was independent on the recording condition (Figure 2b), suggesting that Thio-THIP-responding receptors close to the synapse are not similarly sensitive to kinase activity as extrasynaptic receptors. $GABA_A$ receptors interact with, among others, gephyrin, GABA receptor associated protein, calreticulin (gC1q-R) and AKAP79/150 through a ~30 AA long domain in the intracellular TM3-TM4 loop (Brandon et al., 2003; Essrich, Lorez, Benson, Fritschy, & Luscher, 1998; Schaerer, Kannenberg, Hunziker, Baumann, & Sigel, 2001; Wang, Bedford, Brandon, Moss, & Olsen, 1999). Receptor anchoring at the synapse requires gephyrin interaction and the binding domain for gephyrin has been mapped in the β-subunits and shown to overlap the S383/S409 (CaMK2 site) and the S408/409/410 (PKA and PKC site) (Kowalczyk et al., 2013; Maric et al., 2017; Maric, Mukherjee, Tretter, Moss, & Schindelin, 2011). Trafficking of $GABA_A$ and glycine receptors is sensitive to calcineurin and PKC activity due in part to phosphorylation of gephyrin (Bannai et al., 2009; Specht et al., 2011; Tyagarajan et al., 2011; Zacchi, Antonelli, & Cherubini, 2014). However, phosphorylation of receptor subunits is likely to also play a role in anchoring to gephyrin, as phosphorylation of the S409 residue in a $GABA_A$ receptor subunit β_1 fragment also reduces the affinity to gephyrin fragments (Maric, personal communication).

4.3 | Gabazine and the constitutive current in rodent dentate gyrus granule cells (DGGCs)

The two orthosteric $GABA_A$ receptor antagonists, gabazine and bicuculline, exert different effects against spontaneously active $GABA_A$ receptors:- bicuculline shuts spontaneously active receptors (Birnir et al., 2000) and is termed an inverse agonist whereas gabazine is ineffective towards these (McCartney et al., 2007; Wlodarczyk et al., 2013) and is termed a neutral antagonist. The constitutive current in recording condition *b* can be closed by bicuculline and possibly displaced by gabazine for receptors to resume constitutive gating (see McCartney et al., 2007; Wlodarczyk et al., 2013 and Figure 3b). However, since gabazine is capable of introducing this current by itself, but only under conditions of shut constitutive channels, we conclude that the tonic current density is the result of an action by gabazine at a receptor associated with a shut channel and not bicuculline displacement. Further, since 20 μM of bicuculline did not in the least affect the magnitude of current induced by gabazine (Figure 3b), this would argue against that bicuculline compete with gabazine to reverse this effect. Similar to the effect of Thio-THIP in recording condition *b* described above, the effect of gabazine was hidden in the already active constitutive current. This effect of gabazine in DGGCs was picrotoxin- and DS2-sensitive, completely δ-subunit dependent, TPMPA-insensitive, partially β_1-dependent and displayed an EC_{50} of 2.1 μM. We have summarized the essence of this relation between constitutive current and agonist induced current in Figure 6. Since the mechanism of PKC mediated $GABA_A$ receptor desensitization both generate spontaneous current, but also limit agonist mediated current, it is not clear how the net excitability is affected. However, in the condition of desensitized extrasynaptic receptors, the effect of GABA from inhibition of uptake or release from neurogliaform interneurons is likely diminished. However, we were unable to demonstrate that $\alpha_4\beta_{1/3}\delta$ receptors expressed in HEK-293 cells display a gabazine-induced current when measured by the FMP assay (Figure 4a–f). Nor were we able to see spontaneous activity in recombinant $\alpha_4\beta_1\delta$ receptors when recorded from in conventional patch clamp mode in similar conditions to condition *b* (Figure 4g, h). It is possible that intracellular components acting through the TM3-TM4 loop at β-subunits mediating the effects of gabazine in DGGCs are missing in the HEK-293 cells, as argued by the relative insensitivity of $GABA_A$ receptors to CaMK2 modulation in HEK-293 cells (Houston & Smart, 2006). Since gabazine had no effect on the tonic current density induced by Thio-THIP in $\beta_1^{+/+}$ mice, but reduced the tonic current density by Thio-THIP in $\beta_1^{-/-}$ mice (Figure 5c, d), we conclude that, in addition to the δ-subunits, the β_1-subunit-containing receptors are also involved in the response by gabazine, but not exclusively so. We hypothesize that phosphorylation of the receptor induces a state of the receptor with a high degree of spontaneous activity. Gabazine can, in the absence of phosphorylation, induce a similar state of high spontaneous activity. We believe that some of the effects of gabazine alone on DGGCs have been observed by others before us, but not subjected to methodological analysis. This may in part be because the connection to the constitutive gating was not assessed. However, specific methodologies used in the field, such as recordings at different temperatures, adding GABA to the ACSF, including or excluding TTX and using intracellular solutions of different Ca-chelating capacity here are confounders which can be obviated to determine the effect of gabazine on $\alpha_4\beta_{1/3}\delta$ in DGGCs. Furthermore, we suggest that the relationship between PKC and desensitized receptors implies that the use PKC activators or inhibitors in the presence of GABA and desensitized $GABA_A$ receptors can lead to ambiguous interpretation of data.

In conclusion, we have described the existence of kinase-dependent behaviour of δ-subunit-containing $GABA_A$ receptors

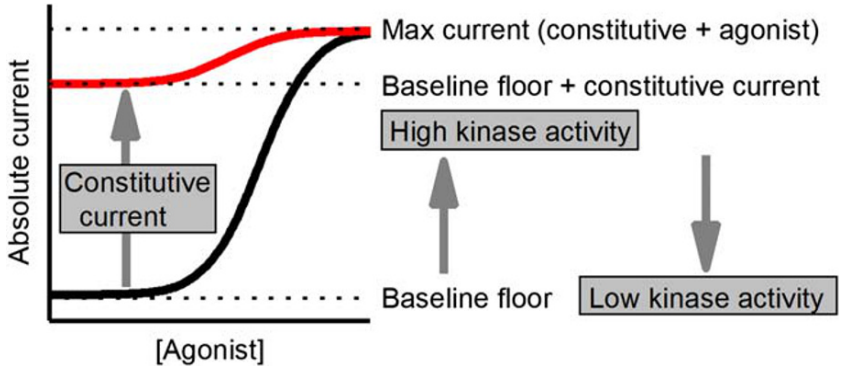

FIGURE 6 A graphical illustration of the relationship between the agonist-induced and the spontaneous current in dentate gyrus granule cells (DGGCs). Central for the model is the observation that the agonist-induced (by Thio-THIP) and the spontaneous current, although mediated by same receptors, are not additive but better described as complimentary. The maximum current gated by a receptor is fixed, irrespective of it being due to spontaneous or ligand-gating, but the baseline floor is set by the constitutive current which is determined by the endogenous kinase activity towards $GABA_A$ receptors: the larger the constitutive current, the less room for agonist induced current. The physiological relevance of this relation may become apparent when considering diseases involving a much increased PKC activity in distinct neurons (e.g. epilepsy or addiction including alcoholism) against which certain GABAergic compounds are surprisingly ineffective. The model is based on data of the present manuscript and those presented by Tang et al. (2010)

that disguises the efficacy of orthosteric agonists and gabazine. This is likely to concern the effects of orthosteric activation of δ-subunit-containing $GABA_A$ receptors in specific pathologies such as epilepsy and addiction including alcoholism (Anstee et al., 2013; Garcia-Pardo, Roger-Sanchez, Rodriguez-Arias, Minarro, & Aguilar, 2016; Kia et al., 2011).

ACKNOWLEDGEMENTS

The authors would like to thank Dr. Javier Martín from the Transgenic Core Facility at the University of Copenhagen for excellent technical assistance with generating the β_1 knockout mouse strain. Further, we are thankful to Dr. Delia Belelli for fruitful discussions and for the generous gift of the δ knockout mouse strain. Dr. Anders Klein is kindly acknowledged for help with animal work. Dr. Uffe Kristiansen's help with patch clamp recordings in HEK cells is much appreciated. This work was supported by funding from the Lundbeck Foundation (grants R133-A12270 to P.W., R192-2015-666 to U.L. and R230-2016-2562 to C.B.F.-P.).

AUTHOR CONTRIBUTION

N.O.D. conceived the study together with P.W., conducted and analysed all slice electrophysiology experiments and was main responsible for writing the manuscript. P.W. conceptualized the studies involving the β_1 knockout mouse strain. C.B.F.-P. performed and analysed whole-cell patch-clamp and FMP experiments on GABA receptors expressed in HEK-293 cells. U.L. performed Western blots and genotyping of transgenic mice together with P.W. P.S. supplied GABA receptor subtype specific antibodies. J.K. and B.F. synthesized THIP and Thio-THIP. P.W. co-wrote the manuscript together with N.O.D. All authors contributed by correcting and proof-reading the manuscript.

CONFLICT OF INTEREST

The authors declare no conflicts of interest.

DECLARATION OF TRANSPARENCY AND SCIENTIFIC RIGOUR

This declaration acknowledges that this paper adheres to the principles for transparent reporting and scientific rigour of preclinical research as stated in the *BJP* guidelines for Natural Product Research, Design and Analysis, Immunoblotting and Immunochemistry, and Animal Experimentation, and as recommended by funding agencies, publishers and other organizations engaged with supporting research.

ORCID

Nils Ole Dalby https://orcid.org/0000-0002-1901-4205
Christina Birkedahl Falk-Petersen https://orcid.org/0000-0001-8576-9406
Ulrike Leurs https://orcid.org/0000-0002-8828-3505
Petra Scholze https://orcid.org/0000-0003-4984-6034
Jacob Krall https://orcid.org/0000-0002-7452-3459
Bente Frølund https://orcid.org/0000-0001-5476-6288
Petrine Wellendorph https://orcid.org/0000-0002-5455-8013

REFERENCES

Alexander, S. P. H., Mathie, A., Peters, J. A., Veale, E. L., Striessnig, J., Kelly, E., … CGTP Collaborators. (2019). THE CONCISE GUIDE TO PHARMACOLOGY 2019/20: Ion channels. *British Journal of Pharmacology*, *176*, S142–S228. https://doi.org/10.1111/bph.14749

Alexander, S. P. H., Roberts, R. E., Broughton, B. R. S., Sobey, C. G., George, C. H., Stanford, S. C., … Ahluwalia, A. (2018). Goals and practicalities of immunoblotting and immunohistochemistry: A guide for submission to the British Journal of Pharmacology. *British Journal of Pharmacology*, *175*, 407–411. https://doi.org/10.1111/bph.14112

Anstee, Q. M., Knapp, S., Maguire, E. P., Hosie, A. M., Thomas, P., Mortensen, M., … Thomas, H. C. (2013). Mutations in the Gabrb1 gene promote alcohol consumption through increased tonic inhibition. *Nature Communications*, *4*, 1–11. https://doi.org/10.1038/ncomms3816

Bannai, H., Levi, S., Schweizer, C., Inoue, T., Launey, T., Racine, V., … Triller, A. (2009). Activity-dependent tuning of inhibitory neurotransmission based on $GABA_AR$ diffusion dynamics. *Neuron*, *62*, 670–682. https://doi.org/10.1016/j.neuron.2009.04.023

Birnir, B., Everitt, A. B., Lim, M. S., & Gage, P. W. (2000). Spontaneously opening $GABA_A$ channels in CA1 pyramidal neurones of rat hippocampus. *The Journal of Membrane Biology*, *174*, 21–29. https://doi.org/10.1007/s002320001028

Brandon, N. J., Delmas, P., Kittler, J. T., McDonald, B. J., Sieghart, W., Brown, D. A., … Moss, S. J. (2000). $GABA_A$ receptor phosphorylation and functional modulation in cortical neurons by a protein kinase C-dependent pathway. *The Journal of Biological Chemistry*, *275*, 38,856–38,862. https://doi.org/10.1074/jbc.M004910200

Brandon, N. J., Jovanovic, J. N., Colledge, M., Kittler, J. T., Brandon, J. M., Scott, J. D., & Moss, S. J. (2003). A-kinase anchoring protein 79/150 facilitates the phosphorylation of $GABA_A$ receptors by cAMP-dependent protein kinase via selective interaction with receptor β subunits. *Molecular and Cellular Neurosciences*, *22*, 87–97. https://doi.org/10.1016/s1044-7431(02)00017-9

Bright, D. P., Renzi, M., Bartram, J., McGee, T. P., MacKenzie, G., Hosie, A. M., … Brickley, S. G. (2011). Profound desensitization by ambient GABA limits activation of δ-containing $GABA_A$ receptors during spillover. *The Journal of Neuroscience*, *31*, 753–763. https://doi.org/10.1523/JNEUROSCI.2996-10.2011

Bright, D. P., & Smart, T. G. (2013). Protein kinase C regulates tonic $GABA_A$ receptor-mediated inhibition in the hippocampus and thalamus. *The European Journal of Neuroscience*, *38*, 3408–3423. https://doi.org/10.1111/ejn.12352

Chandra, D., Jia, F., Liang, J., Peng, Z., Suryanarayanan, A., Werner, D. F., … Homanics, G. E. (2006). $GABA_A$ receptor α4 subunits mediate extrasynaptic inhibition in thalamus and dentate gyrus and the action of gaboxadol. *Proceedings of the National Academy of Sciences of the United States of America*, *103*, 15,230–15,235. https://doi.org/10.1073/pnas.0604304103

Chemin, J., Mezghrani, A., Bidaud, I., Dupasquier, S., Marger, F., Barrere, C., … Lory, P. (2007). Temperature-dependent modulation of CaV3 T-type calcium channels by protein kinases C and A in mammalian cells. *The Journal of Biological Chemistry*, *282*, 32,710–32,718. https://doi.org/10.1074/jbc.M702746200

Curtis, M. J., Alexander, S., Cirino, G., Docherty, J. R., George, C. H., Giembycz, M. A., … Ahluwalia, A. (2018). Experimental design and analysis and their reporting II: Updated and simplified guidance for authors and peer reviewers. *British Journal of Pharmacology*, *175*, 987–993. https://doi.org/10.1111/bph.14153

Essrich, C., Lorez, M., Benson, J. A., Fritschy, J. M., & Luscher, B. (1998). Postsynaptic clustering of major $GABA_A$ receptor subtypes requires the γ2 subunit and gephyrin. *Nature Neuroscience*, *1*, 563–571. https://doi.org/10.1038/2798

Falk-Petersen, C. B., Sogaard, R., Madsen, K. L., Klein, A. B., Frolund, B., & Wellendorph, P. (2017). Development of a robust mammalian cell-based assay for studying recombinant $\alpha_4\beta_{1/3}\delta$ $GABA_A$ receptor subtypes. *Basic & Clinical Pharmacology & Toxicology*, *121*, 119–129. https://doi.org/10.1111/bcpt.12778

Farrant, M., & Nusser, Z. (2005). Variations on an inhibitory theme: phasic and tonic activation of $GABA_A$ receptors. *Nature Reviews. Neuroscience*, *6*, 215–229. https://doi.org/10.1038/nrn1625

Garcia-Pardo, M. P., Roger-Sanchez, C., Rodriguez-Arias, M., Minarro, J., & Aguilar, M. A. (2016). Pharmacological modulation of protein kinases as a new approach to treat addiction to cocaine and opiates. *European Journal of Pharmacology*, *781*, 10–24. https://doi.org/10.1016/j.ejphar.2016.03.065

Glykys, J., & Mody, I. (2007). Activation of $GABA_A$ receptors: Views from outside the synaptic cleft. *Neuron*, *56*, 763–770. https://doi.org/10.1016/j.neuron.2007.11.002

Harding, S. D., Sharman, J. L., Faccenda, E., Southan, C., Pawson, A. J., Ireland, S., … NC-IUPHAR. (2018). The IUPHAR/BPS Guide to PHARMACOLOGY in 2018: Updates and expansion to encompass the new guide to IMMUNOPHARMACOLOGY. *Nucleic Acids Research*, *46*, D1091–D1106. https://doi.org/10.1093/nar/gkx1121

Herd, M. B., Haythornthwaite, A. R., Rosahl, T. W., Wafford, K. A., Homanics, G. E., Lambert, J. J., & Belelli, D. (2008). The expression of $GABA_A\beta$ subunit isoforms in synaptic and extrasynaptic receptor populations of mouse dentate gyrus granule cells. *The Journal of Physiology*, *586*, 989–1004. https://doi.org/10.1113/jphysiol.2007.146746

Hoestgaard-Jensen, K., Dalby, N. O., Krall, J., Hammer, H., Krogsgaard-Larsen, P., Frolund, B., & Jensen, A. A. (2014). Probing $\alpha_4\beta\delta$ $GABA_A$ receptor heterogeneity: Differential regional effects of a functionally selective $\alpha_4\beta_1\delta/\alpha_4\beta_3\delta$ receptor agonist on tonic and phasic inhibition in rat brain. *The Journal of Neuroscience*, *34*, 16,256–16,272. https://doi.org/10.1523/JNEUROSCI.1495-14.2014

Houston, C. M., Lee, H. H., Hosie, A. M., Moss, S. J., & Smart, T. G. (2007). Identification of the sites for CaMK-II-dependent phosphorylation of $GABA_A$ receptors. *The Journal of Biological Chemistry*, *282*, 17,855–17,865. https://doi.org/10.1074/jbc.M611533200

Houston, C. M., & Smart, T. G. (2006). CaMK-II modulation of $GABA_A$ receptors expressed in HEK293, NG108-15 and rat cerebellar granule neurons. *The European Journal of Neuroscience*, *24*, 2504–2514. https://doi.org/10.1111/j.1460-9568.2006.05145.x

Jensen, M. L., Wafford, K. A., Brown, A. R., Belelli, D., Lambert, J. J., & Mirza, N. R. (2013). A study of subunit selectivity, mechanism and site of action of the δ selective compound 2 (DS2) at human recombinant and rodent native $GABA_A$ receptors. *British Journal of Pharmacology*, *168*, 1118–1132. https://doi.org/10.1111/bph.12001

Kia, A., Ribeiro, F., Nelson, R., Gavrilovici, C., Ferguson, S. S., & Poulter, M. O. (2011). Kindling alters neurosteroid-induced modulation of phasic and tonic $GABA_A$ receptor-mediated currents: Role of phosphorylation. *Journal of Neurochemistry*, *116*, 1043–1056. https://doi.org/10.1111/j.1471-4159.2010.07156.x

Kilkenny, C., Browne, W., Cuthill, I. C., Emerson, M., & Altman, D. G. (2010). Animal research: Reporting in vivo experiments: The ARRIVE guidelines. *British Journal of Pharmacology*, *160*, 1577–1579.

Kowalczyk, S., Winkelmann, A., Smolinsky, B., Forstera, B., Neundorf, I., Schwarz, G., & Meier, J. C. (2013). Direct binding of $GABA_A$ receptor β2 and β3 subunits to gephyrin. *The European Journal of Neuroscience*, *37*, 544–554. https://doi.org/10.1111/ejn.12078

Krehan, D., Frolund, B., Ebert, B., Nielsen, B., Krogsgaard-Larsen, P., Johnston, G. A., & Chebib, M. (2003). Aza-THIP and related analogues of THIP as GABA C antagonists. *Bioorganic & Medicinal Chemistry*, *11*, 4891–4896. https://doi.org/10.1016/j.bmc.2003.09.016

Lee, V., & Maguire, J. (2014). The impact of tonic $GABA_A$ receptor-mediated inhibition on neuronal excitability varies across brain region and cell type. *Front Neural Circuits*, *8*, 1–27. https://doi.org/10.3389/fncir.2014.00003

Maric, H. M., Hausrat, T. J., Neubert, F., Dalby, N. O., Doose, S., Sauer, M., … Strømgaard, K. (2017). Gephyrin-binding peptides visualize postsynaptic sites and modulate neurotransmission. *Nature Chemical Biology*, *13*, 153–160. https://doi.org/10.1038/nchembio.2246

Maric, H. M., Mukherjee, J., Tretter, V., Moss, S. J., & Schindelin, H. (2011). Gephyrin-mediated γ-aminobutyric acid type A and glycine receptor clustering relies on a common binding site. *The Journal of Biological Chemistry*, *286*, 42,105–42,114. https://doi.org/10.1074/jbc.M111.303412

Martenson, J. S., Yamasaki, T., Chaudhury, N. H., Albrecht, D., & Tomita, S. (2017). Assembly rules for $GABA_A$ receptor complexes in the brain. *eLife*, *6*, 1–18. https://doi.org/10.7554/eLife.27443

McCartney, M. R., Deeb, T. Z., Henderson, T. N., & Hales, T. G. (2007). Tonically active $GABA_A$ receptors in hippocampal pyramidal neurons exhibit constitutive GABA-independent gating. *Molecular Pharmacology*, *71*, 539–548. https://doi.org/10.1124/mol.106.028597

Mihalek, R. M., Banerjee, P. K., Korpi, E. R., Quinlan, J. J., Firestone, L. L., Mi, Z. P., … Homanics, G. E. (1999). Attenuated sensitivity to neuroactive steroids in γ-aminobutyrate type A receptor δ subunit knockout mice. *Proceedings of the National Academy of Sciences of the United States of America*, *96*, 12,905–12,910. https://doi.org/10.1073/pnas.96.22.12905

Olsen, R. W., & Sieghart, W. (2008). International Union of Pharmacology. LXX. Subtypes of γ-aminobutyric $acid_A$ receptors: Classification on the basis of subunit composition, pharmacology, and function. Update. *Pharmacological Reviews*, *60*, 243–260. https://doi.org/10.1124/pr.108.00505

Othman, N. A., Gallacher, M., Deeb, T. Z., Baptista-Hon, D. T., Perry, D. C., & Hales, T. G. (2012). Influences on blockade by t-butylbicyclo-phosphoro-thionate of $GABA_A$ receptor spontaneous gating, agonist activation and desensitization. *The Journal of Physiology*, *590*, 163–178. https://doi.org/10.1113/jphysiol.2011.213249

Overstreet-Wadiche, L., & McBain, C. J. (2015). Neurogliaform cells in cortical circuits. *Nature Reviews. Neuroscience*, *16*, 458–468. https://doi.org/10.1038/nrn3969

Schaerer, M. T., Kannenberg, K., Hunziker, P., Baumann, S. W., & Sigel, E. (2001). Interaction between $GABA_A$ receptor β subunits and the multifunctional protein gC1q-R. *The Journal of Biological Chemistry*, *276*, 26,597–26,604. https://doi.org/10.1074/jbc.M102534200

Specht, C. G., Grunewald, N., Pascual, O., Rostgaard, N., Schwarz, G., & Triller, A. (2011). Regulation of glycine receptor diffusion properties and gephyrin interactions by protein kinase C. *The EMBO Journal*, *30*, 3842–3853. https://doi.org/10.1038/emboj.2011.276

Sperk, G., Schwarzer, C., Tsunashima, K., Fuchs, K., & Sieghart, W. (1997). $GABA_A$ receptor subunits in the rat hippocampus I: Immunocytochemical distribution of 13 subunits. *Neuroscience*, *80*, 987–1000. https://doi.org/10.1016/s0306-4522(97)00146-2

Tang, X., Hernandez, C. C., & Macdonald, R. L. (2010). Modulation of spontaneous and GABA-evoked tonic α4β3δ and α4β3γ2L $GABA_A$ receptor currents by protein kinase A. *Journal of Neurophysiology*, *103*, 1007–1019. https://doi.org/10.1152/jn.00801.2009

Tyagarajan, S. K., Ghosh, H., Yevenes, G. E., Nikonenko, I., Ebeling, C., Schwerdel, C., … Fritschy, J. M. (2011). Regulation of GABAergic synapse formation and plasticity by GSK3β-dependent phosphorylation of gephyrin. *Proceedings of the National Academy of Sciences of the United States of America*, *108*, 379–384. https://doi.org/10.1073/pnas.1011824108

Wang, H., Bedford, F. K., Brandon, N. J., Moss, S. J., & Olsen, R. W. (1999). $GABA_A$-receptor-associated protein links $GABA_A$ receptors and the cytoskeleton. *Nature*, *397*, 69–72. https://doi.org/10.1038/16264

Wei, W., Zhang, N., Peng, Z., Houser, C. R., & Mody, I. (2003). Perisynaptic localization of δ subunit-containing $GABA_A$ receptors and their activation by GABA spillover in the mouse dentate gyrus. *The Journal of Neuroscience*, *23*, 10,650–10,661. https://doi.org/10.1523/JNEUROSCI.23-33-10650.2003

Wlodarczyk, A. I., Sylantyev, S., Herd, M. B., Kersante, F., Lambert, J. J., Rusakov, D. A., … Walker, M. C. (2013). GABA-independent $GABA_A$ receptor openings maintain tonic currents. *The Journal of Neuroscience*, *33*, 3905–3914. https://doi.org/10.1523/JNEUROSCI.4193-12.2013

Zacchi, P., Antonelli, R., & Cherubini, E. (2014). Gephyrin phosphorylation in the functional organization and plasticity of GABAergic synapses. *Frontiers in Cellular Neuroscience*, *8*, 1–9. https://doi.org/10.3389/fncel.2014.00103

Zhang, N., Wei, W., Mody, I., & Houser, C. R. (2007). Altered localization of $GABA_A$ receptor subunits on dentate granule cell dendrites influences tonic and phasic inhibition in a mouse model of epilepsy. *The Journal of Neuroscience*, *27*, 7520–7531. https://doi.org/10.1523/JNEUROSCI.1555-07.2007

How to cite this article: Dalby NO, Falk-Petersen CB, Leurs U, et al. Silencing of spontaneous activity at α4β1/3δ $GABA_A$ receptors in hippocampal granule cells reveals different ligand pharmacology. *Br J Pharmacol*. 2020;177:3975–3990. https://doi.org/10.1111/bph.15146